Tailored bistability in mechanically pre-stressed laminated composites through planform design

Chillara, Venkata Siva, Dapino, Marcelo

Venkata Siva C. Chillara, Marcelo J. Dapino, "Tailored bistability in mechanically pre-stressed laminated composites through planform design," Proc. SPIE 10968, Behavior and Mechanics of Multifunctional Materials XIII, 1096811 (29 March 2019); doi: 10.1117/12.2514331

SPIE.

Event: SPIE Smart Structures + Nondestructive Evaluation, 2019, Denver, Colorado, United States

Tailored Bistability in Mechanically-Prestressed Laminated Composites through Planform Design

Venkata Siva C. Chillara* and Marcelo J. Dapino

NSF IUCRC on Smart Vehicle Concepts,
Department of Mechanical and Aerospace Engineering,
The Ohio State University, Columbus, OH 43210

ABSTRACT

Bistable composites are attractive for morphing structures because they can hold deformed shapes without actuation and can be driven by compact, embedded smart actuators such as piezoelectric laminae and shape memory alloys. Mechanically-prestressed bistable composites exhibit weakly-coupled cylindrical shapes when their prestressed laminae are orthogonal to each other. High-order analytical models have been developed to model the stability and actuation of mechanically-prestressed composites with two sources of residual stress. Based on these models, this paper presents a study on the effect of planform shape on shape-bifurcation phenomena in bistable plates. A high-order analytical model is presented and the shapes of composites with linearly-tapered planform are calculated. Model-based parametric studies are presented to calculate the sensitivity of stable shapes and actuation forces to variations in planform taper, spatial positions of the prestressed layers, and aspect ratio. The results guide the selection of geometric parameters for the design of bistable composites.

Keywords: Bistable, morphing, high-order model, actuation, prestress, reinforced elastomer

1. INTRODUCTION

Laminated composites, with bistability arising from thermal or mechanical prestress, are attractive for shape morphing because actuation is required only for transition between deformed shapes.[1–3] Bistable elements in a structure enable drastic and rapid changes in shape in an energy-efficient manner. Examples of applications include air ducts,[4] winglets,[5] automotive fender skirts,[6] and structural load-alleviation devices.[7] The deformed shapes of bistable laminates are a function of their planform geometry, size, and the material properties of the constituent laminae.[8]

The morphing characteristics of bistable composites with rectangular planform have been studied through modeling and experiments. The composites have been modeled as laminated plates and their deformed shapes have been calculated using strain energy minimization. While the assumption of constant curvature (second-order displacement polynomial) is sufficient to calculate stable shapes, higher-order polynomials are required for accurate calculation of actuation loads (known as snap-through).[9,10] Several designs of bistable laminates have been presented based on tailored material properties, ply orientations,[11] inclusion of hybrid laminae,[12] and non-square planform shapes.[13] However, the effect of planform shapes on the laminates' domain of bistability and actuation requirements is yet to be fully understood.

This paper presents a high-order analytical model for bistable composites with non-square geometries. Mechanically-prestressed laminated composites are considered in the analyses. These composites comprise an isotropic core material sandwiched between two mechanically-prestressed elastomeric matrix composites (EMC). The EMCs are slender elastomeric strips reinforced with unidirectional fibers along the width; the reinforcement enables zero in-plane Poisson's ratio. Prestress is applied by stretching each strip along its length and laminating it to the core in the stretched state. When the EMCs are orthogonal to each other, the resulting stable shapes

*Further author information: (Send correspondence to V.S.C.)
V.S.C.: E-mail: chillara.1@osu.edu
M.J.D.: E-mail: dapino.1@osu.edu

Behavior and Mechanics of Multifunctional Materials XIII, edited by Hani E. Naguib, Proc. of SPIE
Vol. 10968, 1096811 · © 2019 SPIE · CCC code: 0277-786X/19/$18 · doi: 10.1117/12.2514331

are weakly-coupled; a change in prestress in one EMC affects only one shape. Analytical modeling, construction details, and experimental validation of mechanically-prestressed composites have been discussed by Chillara and Dapino.[3,10] It is expected that an asymmetry in planform geometry alters the composite's stable shapes and snap-through loads. The shift in performance is characterized through a sensitivity study and mechanisms for compensating for the shift, such as changing the relative positions of the EMCs and actuation forces, are investigated.

2. ANALYTICAL MODEL

A mechanically-prestressed bistable composite is modeled based on the geometry shown in Figure 1. The core layer has a trapezoidal shape whereas the EMCs are rectangular strips. Prestressed EMCs in X and Y directions are referred as 0° and 90° EMCs, respectively. The composite is modeled based on classical laminate theory in conjunction with von Karman's hypothesis. Displacements are described using unknown polynomial functions and strain energy is calculated as a function of displacements. Seventh-order polynomials are chosen for accurate calculation of transition points related to loss in bistability and snap-through between shapes; displacement functions and areal dimensions are non-dimensionalized to improve numerical conditioning. Work done by actuation forces is computed using the variational principle. The net energy is minimized using the Rayleigh-Ritz technique to calculate stable shapes as a function of actuation forces.

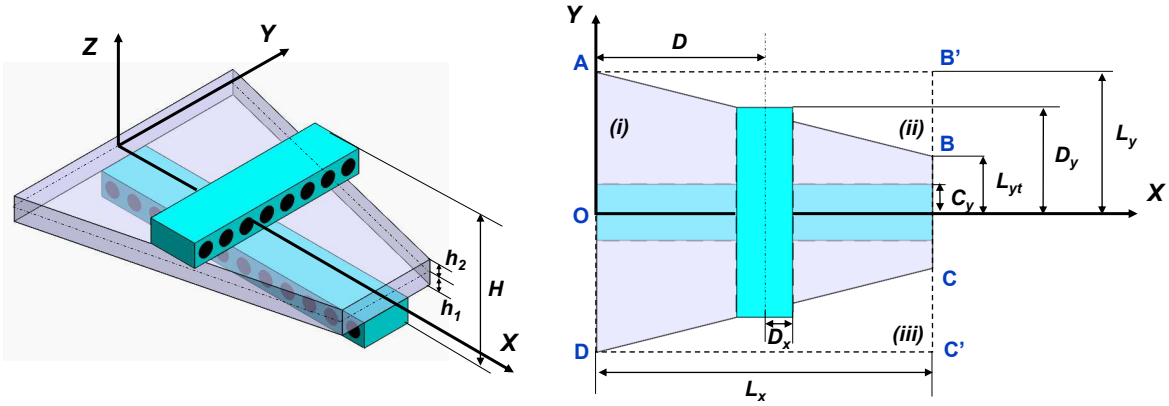

Figure 1: Schematic representation of a mechanically-prestressed bistable laminate.

The ratio of EMC width to core width is defined as:

$$\alpha_0 = \frac{2D_x}{L_x}, \quad \alpha_{90} = \frac{C_y}{L_y}. \tag{1}$$

The composite, shown in Figure 1, is assumed to be a trapezoid that is symmetric about the X axis. It is clamped at the midpoint (O) of side AD. The 90° EMC is symmetric about the X axis and spans the length of the core whereas the 0° EMC is parallel to the Y axis and spans the width of the core at a given distance D from the X axis. Taper (ω) is defined as:

$$\omega = \frac{L_y - L_{yt}}{L_x}. \tag{2}$$

The minimum value of ω is zero, whereas the maximum value is a function of the aspect ratio L_y/L_x.

The strain energy (Φ_c) of the tapered core $ABCD$ is obtained by subtracting the energy in the triangular regions ABB' and DCC' from the energy in the rectangle $AB'C'D$ (Figure 1). It is expressed in terms of non-dimensionalized coordinates $\tilde{x} = x/L_x$ and $\tilde{y} = y/L_y$ as:

$$\Phi_c = \left(\int_0^1 \int_{-1}^1 \phi_c \, \mathrm{d}\tilde{y} \, \mathrm{d}\tilde{x} \right) - \left(\int_0^1 \int_{1-\omega\tilde{x}}^1 \phi_c \, \mathrm{d}\tilde{y} \, \mathrm{d}\tilde{x} \right) - \left(\int_0^1 \int_{-1}^{\omega\tilde{x}-1} \phi_c \, \mathrm{d}\tilde{y} \, \mathrm{d}\tilde{x} \right). \tag{3}$$

The integrand ϕ_c in (3) is defined as:

$$\phi_{\mathrm{c}} = \int_{h_1}^{h_2} \left(\frac{1}{2} Q_{11}^{(c)} \epsilon_x^2 + Q_{12}^{(c)} \epsilon_x \epsilon_y + \frac{1}{2} Q_{22}^{(c)} \epsilon_y^2 + + Q_{16}^{(c)} \epsilon_x \gamma_y + Q_{26}^{(c)} \epsilon_y \gamma_y + \frac{1}{2} Q_{66}^{(c)} \gamma_{xy}^2 \right) \mathrm{d}z, \tag{4}$$

where $Q_{ij}, \{i, j = 1, 2, 6\}$ are the plane stress-reduced stiffnesses and ϵ_x, ϵ_y, and γ_{xy} are the strains of the composite.[14] The strain energies Φ_{90} and Φ_0 of the 90° and 0° EMCs, respectively, are computed as:

$$\Phi_{90} = \int_0^1 \int_{-\alpha_{90}}^{\alpha_{90}} \int_{-\frac{H}{2}}^{h_1} \left(\frac{p_1}{5} (\epsilon_{90} - \epsilon_x)^5 + \frac{p_2}{4} (\epsilon_{90} - \epsilon_x)^4 + \frac{p_3}{3} (\epsilon_{90} - \epsilon_x)^3 + \frac{p_4}{2} (\epsilon_{90} - \epsilon_x)^2 + \frac{1}{2} Q_{22}^{(90)} \epsilon_y^2 + \frac{1}{2} Q_{66}^{(90)} \gamma_{xy}^2 \right) \mathrm{d}\tilde{z}\, \mathrm{d}\tilde{y}\, \mathrm{d}\tilde{x}, \tag{5}$$

$$\Phi_0 = \int_{D'-\alpha_0}^{D'+\alpha_0} \int_{-1}^{1} \int_{h_2}^{\frac{H}{2}} \left(\frac{1}{2} Q_{11}^{(0)} \epsilon_x^2 + \frac{p_1}{5} (\epsilon_0 - \epsilon_y)^5 + \frac{p_2}{4} (\epsilon_0 - \epsilon_y)^4 + \frac{p_3}{3} (\epsilon_0 - \epsilon_y)^3 + \frac{p_4}{2} (\epsilon_0 - \epsilon_y)^2 + \frac{1}{2} Q_{66}^{(0)} \gamma_{xy}^2 \right) \mathrm{d}\tilde{z}\, \mathrm{d}\tilde{y}\, \mathrm{d}\tilde{x}, \tag{6}$$

where ϵ_{90} and ϵ_0 are the prestrains applied to the 90° and 0° EMCs, respectively. The coefficients p_1 through p_4 are those of a quartic polynomial that describes the nonlinear stress function of an EMC with zero in-plane Poisson's ratio. These coefficients, shown in Table 1, pertain to a polynomial fit of a stress-strain curve measured through a uniaxial tensile test. The total strain energy (Φ) of the system is the sum of the strain energies of the constituent layers:

$$\Phi = \Phi_{\mathrm{c}} + \Phi_{90} + \Phi_0. \tag{7}$$

Table 1: Coefficients of a nonlinear stress function of an EMC with zero in-plane Poisson's ratio obtained from a uniaxial tensile test.

p_1	p_2	p_3	p_4
-0.698 x 10^6	2.29 x 10^6	-2.306 x 10^6	1.598 x 10^6

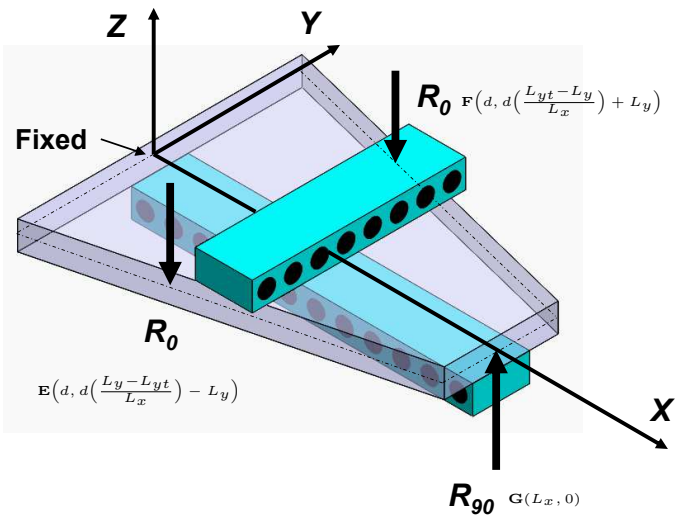

Figure 2: Schematic representation of the actuation forces on the composite.

Snap-through between stable shapes is modeled using transverse external forces R_{90} and R_0 as shown in Figure 2. For example, $R_{90} \neq 0$ and $R_0 = 0$ if the initial stable shape is curved about the Y axis. Variational work

done by the actuation forces is written as:

$$W = R_0 w_0^{(E)} + R_0 w_0^{(F)} + R_{90} w_0^{(G)} \tag{8}$$

Displacements of the mid-plane, described using complete seventh-order polynomials, are of the form:

$$\tilde{u}_0 = \sum_{q=0}^{7}\sum_{p=0}^{q} b_{p,q-p}\tilde{x}^p\tilde{y}^{p-q}, \quad \tilde{v}_0 = \sum_{q=0}^{7}\sum_{p=0}^{q} c_{p,q-p}\tilde{x}^p\tilde{y}^{p-q}, \quad \tilde{w}_0 = \sum_{q=0}^{7}\sum_{p=0}^{q} d_{p,q-p}\tilde{x}^p\tilde{y}^{p-q}, \tag{9}$$

where $b_{p,q-p}$, $c_{p,q-p}$, and $d_{p,q-p}$ are the unknown coefficients that are to be evaluated. Given that the composite is symmetric about the X axis, $\tilde{v}_0$ is assumed to odd in $\tilde{y}$ and even in $\tilde{x}$. Though the composite lies in the $\tilde{x} > 0$ space, it's displacement can be assumed to be symmetric about the Y axis. This choice does not affect the solution since strain energy is computed only for $\tilde{x} > 0$. Therefore, $\tilde{u}_0$ is odd in $\tilde{x}$ and even in $\tilde{y}$. The out-of-plane displacement $\tilde{w}_0$ is even in $\tilde{x}$ and $\tilde{y}$.

The equilibrium shapes of the composite are obtained as a function of actuation forces by minimizing the net energy using the Rayleigh-Ritz approach:

$$\sum_i \frac{\partial(\Phi - W)}{\partial C_i} = 0, \tag{10}$$

where $C_i = \{b_{p,q-p}, c_{p,q-p}, d_{p,q-p}\}$ for p ranging from 0 to q and q ranging from 0 to 7. The number of coefficients for seventh order polynomials is 29. The expressions for U_T, W, and their partial derivatives are derived in symbolic form using MAPLE. The nonlinear equations resulting from (10) are solved in MATLAB using the Newton-Raphson method.

3. RESULTS AND DISCUSSION

The model presented in section 2 has been experimentally validated by Chillara and Dapino[10] for rectangular laminates. In this section, parametric studies are presented to discuss the effect of planform on the bistable response of the laminate. Material properties and dimensions of the composite are listed in Tables 2 and 3, respectively.

Table 2: Box dimensions of laminae of the modeled prestressed composites.

Lamina	Length (mm)	Width (mm)	Thickness (mm)
90° EMC	152.4	38.1	2.032
Core	152.4	152.4	0.127
0° EMC	38.1	152.4	2.032

Table 3: Material properties of the laminae of the modeled prestressed composites.

Lamina	E_1 (MPa)	E_2 (MPa)	G_{12} (MPa)	ν_{12}	ν_{21}
90° EMC	Nonlinear	0.4	1.2	0	0
Core layer	200,000	200,000	78,125	0.28	0.28
0° EMC	0.4	Nonlinear	1.2	0	0

Stable shapes are calculated as a function of EMC prestrain for laminates with a taper $\omega = 0.5$ (Figure 3). The out-of-plane deflection w_0, measured at $(L_x, 0)$ reduces with a reduction in prestrain ϵ_{90} up to a critical point where the composite loses bistability and settles into a single curved shape (Figure 3(a)); deflection in the resulting monostable composite is a function of ϵ_0. Therefore, for a given prestrain in the 0° EMC, there exists a critical value of prestrain $\epsilon_{90}^{(cr)}$ in the 90° EMC that is required to maintain bistability. Critical prestrain reduces with a reduction in ϵ_0. A similar relationship between EMC prestrains is observed relative to the second stable shape (Figure 3(b)).

Forces corresponding to snap-through and snap-back are calculated for composites with $\omega = 0.5$. Snap-through forces for square composites of side L_x are shown with dashed lines for reference (Figure 4). It is observed that snap-through load corresponding to curvature about the Y axis is the same for tapered and square laminates even though their initial deflections are different (Figure 4(a)). Forces for snap-back are higher in the presence of taper because the moment arm about the mid-plane is lower than in the case of square laminates (Figure 4(b)). Note that a pair of forces, each of magnitude R_0, are applied on the tapered edges (points E and F in Figure 2) at points defined by $d = 0.5L_x$. The increase in snap-through load due to taper could potentially be compensated by shifting the point of application of the forces. Actuation forces required for switching between stable shapes increase with an increase in EMC prestrain.

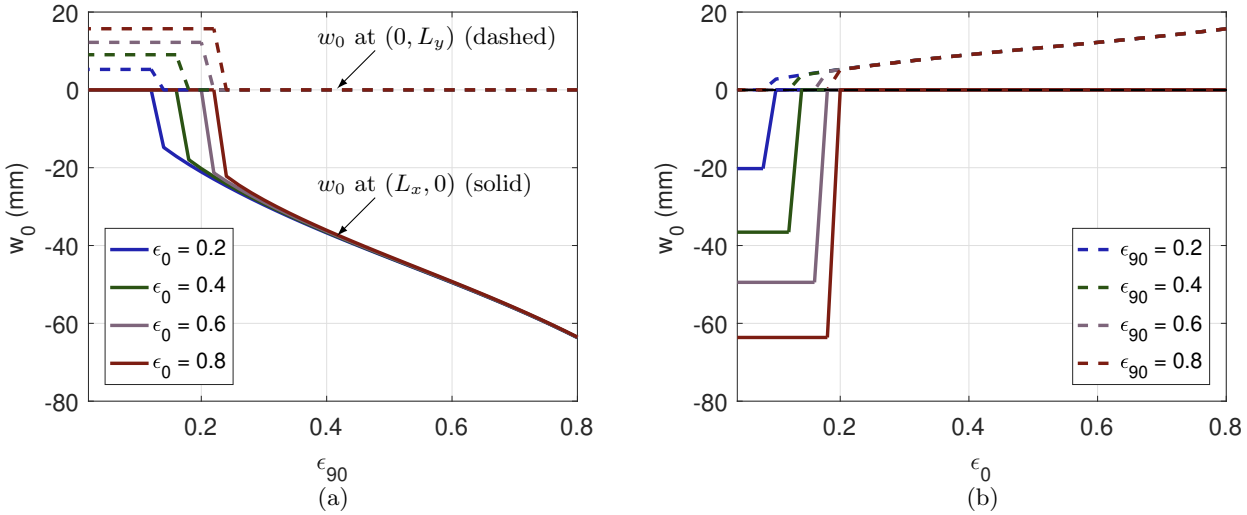

Figure 3: Out-of-plane deflection of the composite corresponding to curvatures about (a) Y axis and (b) X axis. ϵ_{90} and ϵ_0 are the prestrains applied to the 90° and 0° EMCs, respectively

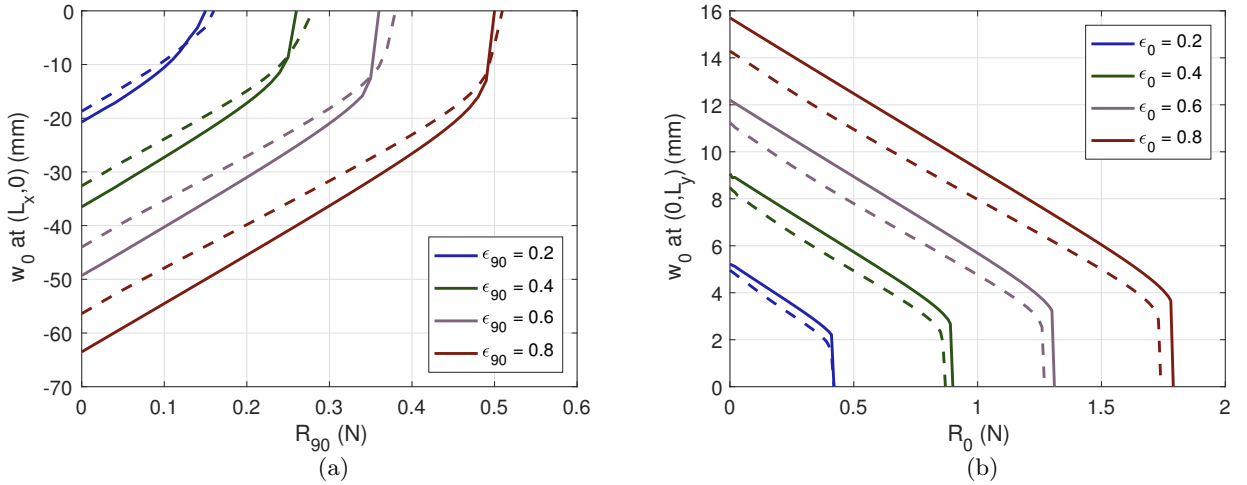

Figure 4: Force-deflection curves showing shape transition in a composite that is initially curved about (a) Y axis and (b) X axis. The dashed and solid lines refer to $\omega = 0$ and $\omega = 0.5$, respectively.

4. SENSITIVITY STUDY

The sensitivity of design parameters is studied relative to two performance metrics, *viz.,* domain of bistability (defined by ϵ_{90}^{cr} and ϵ_{0}^{cr}) and snap through forces defined by R_0 and R_{90}. The parameters analyzed are: planform taper (ω), position of the 0° EMC (D), and position (d) of force (R_0) application on the tapered edges. The tapered composite analyzed has $L_x \triangleq 2L_y = 152.4$ mm.

To study the effect of taper on bistability, tip deflection of a composite curved about the Y axis is shown as a function of prestrain ϵ_{90} (Figure 5(a)); ϵ_0 is kept constant at 1. Critical prestrain ϵ_{90}^{cr} is minimum for a square composite and reaches a maximum as taper is increased. At a given distance along the X axis, the cross-sectional area of the core reduces with an increase in taper, thereby yielding higher curvature (about Y) at the tip $(L_x, 0)$ relative to the root $(0, 0)$. Higher curvature (or w_0) corresponds to higher critical prestrain, as shown in Figure 3(b). Critical prestrain has an inflection point w.r.t. taper such that further increase in taper forces the composite into a monostable curvature about the X axis rather than a higher bistable curvature about the Y axis. Among the critical prestrains, ϵ_{90}^{cr} is more sensitive to taper than ϵ_{0}^{cr} (Figure 5(b)). Such a response can be attributed to a higher deflection, for a given taper, when curved about the Y axis than the X axis.

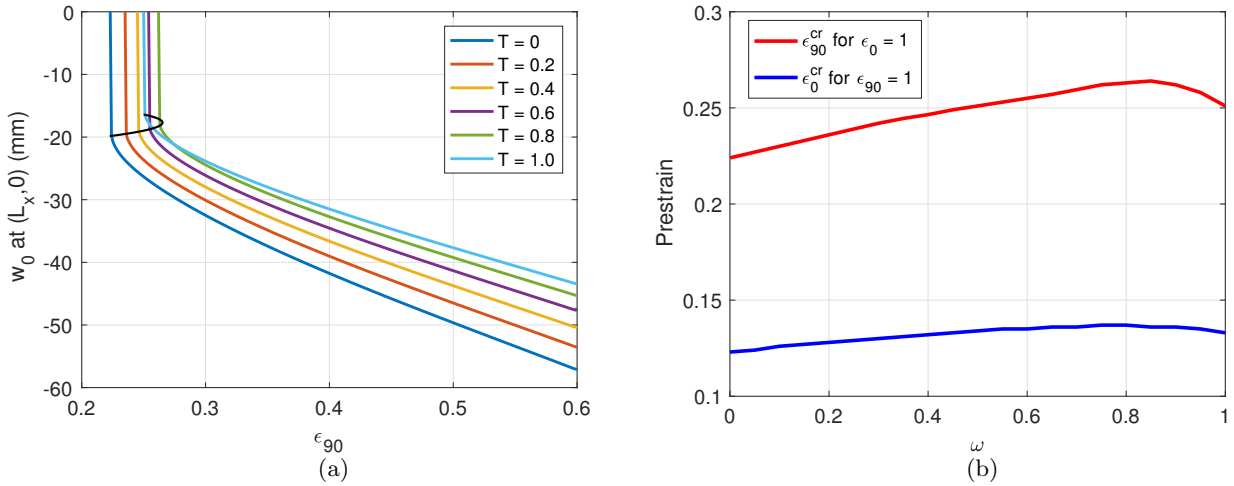

Figure 5: (a) Deflection at $(L_x, 0)$ as a function of prestrain ϵ_{90} for various values for taper. (b) Critical prestrains as a function of taper.

In a composite with non-rectangular planform, the relative position of the EMCs influences bistability. For a trapezoidal geometry, this effect is analyzed by varying the non-dimensionalized distance D/L_x of the 0° EMC along the X axis. Prestrains ϵ_0 and ϵ_{90} are kept constant at 0.4 and 1, respectively. Deflection at $(0, L_y)$ corresponding to curvature about the X axis is shown in Figure 6(a). The sharp change in deflection corresponds to loss in bistability and the existence of a single curvature about the Y axis. These transition points are plotted as a function of taper to obtain the domain of bistability, as represented by the shaded region in Figure 6(b). The lower limit of D/L_x decreases with an increase in taper because the centroid of the trapezoidal core moves closer to the origin. The upper limit of D/L_x increases with taper probably because of high localized curvatures, due to the reduced cross-section, that propagate into a global curvature about the X axis.

The deflection at $(0,L_y)$ of a composite ($\omega = 0.5$) curved about the X axis is calculated as a function of a pair of vertical forces R_0 applied at points E and F (Figure 7). With an increase in the non-dimensionalized distance (d/L_x) of force application, the force required for snap-through increases linearly. Further, the deflection during the snap-through event increases parabolically with an increase in d/L_x. The variation in snap-through force R_0 over taper ranging from 0 to 1 is -4.4% at $d/L_x = 0$ and -10.9% at $d/L_x = 1$ (Figure 8(a)). The corresponding variation in the deflection at snap-through w_0 is -17.7% and -21.9% (Figure 8(b)).

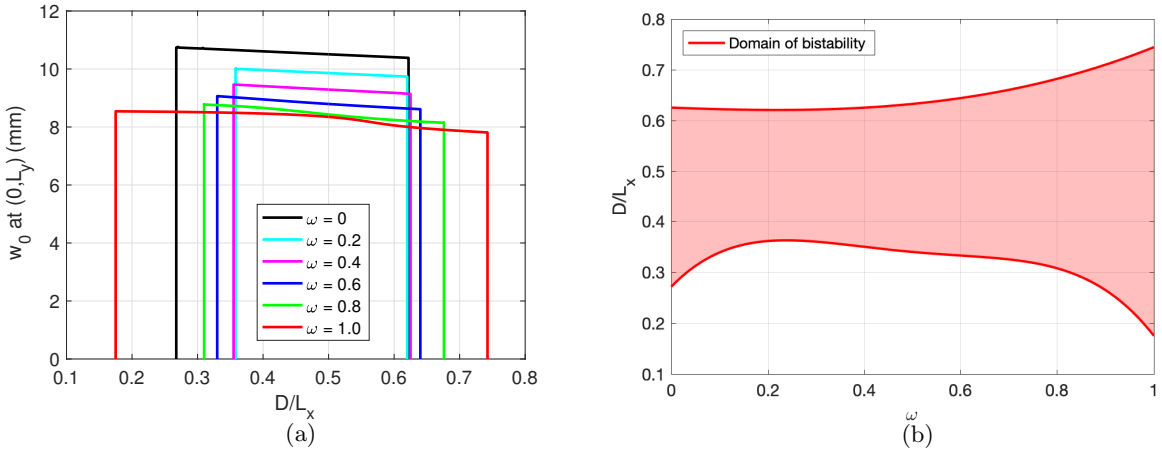

Figure 6: (a) Deflection as a function of the position of the 0° EMC for various values for taper. (b) Range of 0° EMC positions that yield bistability (shown by the shaded region).

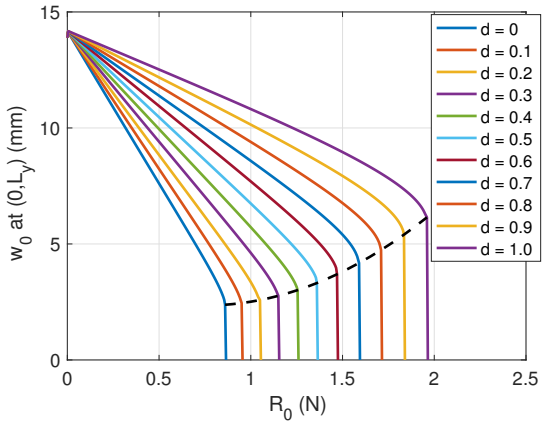

Figure 7: Deflection as a function of snap-through load (R_0) on a composite initially curved about the X axis.

CONCLUDING REMARKS

The response of mechanically-prestressed bistable composites with tapered planform has been modeled in this work. A high-order non-dimensionalized analytical model has been developed to study the sensitivity of design parameters on the stability and actuation requirements of the composites. A trapezoidal planform is considered in the analysis and the stable shapes are compared with those of rectangular laminates. The force requirement for snapping the tapered edges from a flat to curved shape increases with an increase in taper. The sensitivity study presented in this work guides actuator placement and positioning of EMCs for actuating composites with shaped planform, such as winglets, with minimal energy.

ACKNOWLEDGEMENTS

Financial support was provided by the member organizations of the Smart Vehicle Concepts Center, a Phase III National Science Foundation Industry-University Cooperative Research Center (www.SmartVehicleCenter.org) under grant NSF IIP 1738723.

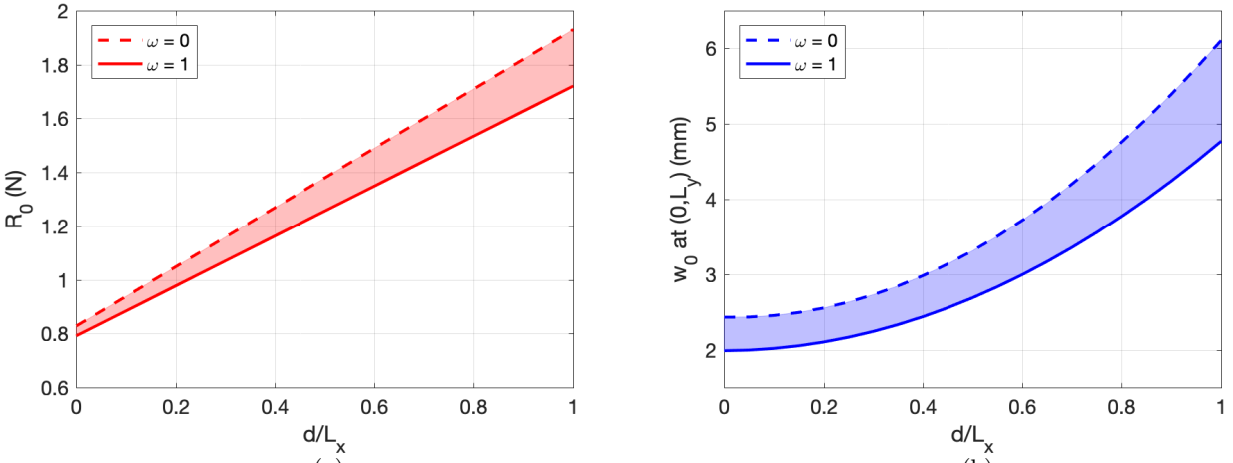

Figure 8: (a) Snap-through load and (b) deflection as a function of non-dimensionalized distance of the force from the YZ plane.

REFERENCES

[1] M. W. Hyer, "Calculations of the room-temperature shapes of unsymmetric laminates," *Journal of Composite Materials*, vol. 15, pp. 296–310, 1981.

[2] S. Daynes, K. D. Potter, and P. M. Weaver, "Bistable prestressed buckled laminates," *Composites Science and Technology*, vol. 68, no. 15–16, pp. 3431–3437, 2008.

[3] V. S. C. Chillara and M. J. Dapino, "Mechanically-prestressed bistable composite laminates with weakly coupled equilibrium shapes," *Composites Part B: Engineering*, vol. 111, pp. 251–260, 2017.

[4] S. Daynes, P. M. Weaver, and J. A. Trevarthen, "A morphing composite air inlet with multiple stable shapes," *Journal of intelligent material systems and structures*, vol. 22, no. 9, pp. 961–973, 2011.

[5] S. Daynes and P. M. Weaver, "Review of shape-morphing automobile structures: concepts and outlook," *Proceedings of the Institution of Mechanical Engineers, Part D: Journal of Automobile Engineering*, vol. 227, no. 11, pp. 1603–1622, 2013.

[6] V. S. C. Chillara, L. M. Headings, R. Tsuruta, E. Itakura, U. Gandhi, and M. J. Dapino, "Shape memory alloy–actuated prestressed composites with application to morphing automotive fender skirts," *Journal of intelligent material systems and structures*, vol. 30, no. 3, pp. 479–494, 2019.

[7] X. Lachenal, S. Daynes, and P. M. Weaver, "A zero torsional stiffness twist morphing blade as a wind turbine load alleviation device," *Smart Materials and Structures*, vol. 22, no. 6, p. 065016, 2013.

[8] M. W. Hyer, "The room-temperature shapes of four-layer unsymmetric cross-ply laminates," *Journal of Composite Materials*, vol. 16, no. 4, pp. 318–340, 1982.

[9] A. Pirrera, D. Avitabile, and P. M. Weaver, "Bistable plates for morphing structures: A refined analytical approach with high-order polynomials," *International Journal of Solids and Structures*, vol. 47, no. 25–26, pp. 3412–3425, 2010.

[10] V. S. C. Chillara and M. J. Dapino, "Stability considerations and actuation requirements in bistable laminated composites," *Composite Structures*, vol. 184, pp. 1062–1070, 2018.

[11] M. L. Dano and M. W. Hyer, "Thermally-induced deformation behavior of unsymmetric laminates," *International Journal of Solids and Structures*, vol. 35, no. 17, pp. 2101–2120, 1998.

[12] S. Daynes and P. Weaver, "Analysis of unsymmetric CFRP–metal hybrid laminates for use in adaptive structures," *Composites Part A: Applied Science and Manufacturing*, vol. 41, no. 11, pp. 1712–1718, 2010.

[13] S. A. Tawfik, D. Stefan Dancila, and E. Armanios, "Planform effects upon the bistable response of cross-ply composite shells," *Composites Part A: Applied Science and Manufacturing*, vol. 42, no. 7, pp. 825–833, 2011.

[14] M. W. Hyer, *Stress analysis of fiber-reinforced composite materials*. DEStech Publications, Inc, 2009.